PHYSICAL REVIEW B VOLUME 60, NUMBER 12 15 SEPTEMBER 1999-II

Experimental evidence for the effect of nonequilibrium acoustic plasmons on carrier relaxation in bulk semiconductors

J. F. Lampin,* F. X. Camescasse, and A. Alexandrou
Laboratoire d'Optique Appliquée, Ecole Polytechnique-Ecole Nationale Supérieure de Techniques Avancées, Unité Mixte de Recherche du Centre National de la Recherche Scientifique No. 7639, Chemin de la Hunière, F-91761 Palaiseau Cedex, France

M. Bonitz
Fachbereich Physik, Universität Rostock, Universitätsplatz 3, D-18051 Rostock, Germany

V. Thierry-Mieg
Laboratoire de Microstructures et de Microélectronique, Unité Propre de Recherche du Centre National de la Recherche Scientifique No. 20, 196, Avenue Henri Ravera, F-92225 Bagneux Cedex, France

(Received 30 April 1999)

We demonstrate experimentally the role of preexisting populations on the relaxation of nonequilibrium carriers in bulk semiconductors: A substantial acceleration is observed for cold preexcited carriers and a slowing down for hot equilibrium carriers. Experiments in doped samples show that holes are predominantly responsible for the acceleration of the thermalization. The observed acceleration (slowing down) is readily explained by favorable (unfavorable) conditions for the excitation of weakly damped nonequilibrium acoustic plasmons. [S0163-1829(99)51336-2]

Fast charged carriers propagating in a solid state or gas plasma may lose a substantial part of their energy due to excitation of plasma oscillations (plasmons). This is well known for three-dimensional (3D) equilibrium plasmas where only the optical plasmon is excited (acoustic modes with linear dispersion are usually strongly damped). In contrast, in nonequilibrium plasmas, additional undamped or even unstable plasmons are possible which may strongly enhance carrier relaxation and transport. This is known from gas plasmas (see, e.g., Ref. 1), however, very little information is available about nonequilibrium plasmons in condensed matter systems. The excitation of coherent optical plasmons has been studied in semiconductors[2] in situations involving nonequilibrium carriers but no experimental evidence for nonequilibrium plasmons has been reported. Theoretical investigations[3,4] have predicted the existence of weakly damped *nonequilibrium acoustic plasmons* in optically excited electron-hole (e-h) plasmas and their importance in accelerating the relaxation. In particular, a drastic dependence on the temperature of *equilibrium carriers existing prior to the injection of a nonequilibrium e-h plasma* was predicted:[3] an acceleration of the relaxation, if the equilibrium population is cold, and a slowing down if it is hot.

A few experimentalists have studied the relaxation dynamics of a nonequilibrium population in the presence of equilibrium carriers,[5–8] which is a situation frequently encountered in devices. However, a comparison between the experimental data is hampered by the fact that they are performed under very different conditions and, to our knowledge, no nonequilibrium plasmon effects have been found up to now.

We here present the first experimental evidence for the existence of nonequilibrium acoustic plasmons in solids and their role in carrier relaxation. We demonstrate the theoretically predicted temperature dependence[3] by measuring the relaxation in the presence of hot and cold equilibrium carriers injected by a prepump under identical conditions, and show that this dependence is directly related to favorable or unfavorable conditions for the excitation of nonequilibrium acoustic plasmons.

In contrast to previous studies, we use a nondegenerate pump-probe configuration[9] that makes it possible to selectively follow the thermalization of the nonequilibrium *electron* distribution: The pump excites electrons from the heavy-hole (HH) and light-hole (LH) valence bands while the probe measures the absorption saturation of the transition from the split-off-hole (SO) valence band (empty of holes) to the conduction band (C). Thus, the effect of the equilibrium populations can be assessed unambiguously without any complications coming from the simultaneous measurement of electron and hole dynamics as in usual experiments.

Recently, considerable progress has been made in the microscopic modelling of carrier relaxation through Coulomb collisions, including dynamic screening[3,10] and femtosecond screening build up.[11] However, with preexcited carriers, screening is largely built up, so simpler Markovian screening models are expected to work well. Indeed, our experimental observations can be fully explained by the plasmon spectrum computed from the Lindhard dielectric function. A very general and intuitive picture is presented which is based on the *total velocity distribution function* of the electron-hole plasma.

The laser setup consists of a Ti:sapphire fs oscillator and a 200-kHz regenerative amplifier (Coherent RegA) followed by an optical parametric amplifier (OPA).[12] For the three-pulse experiments, we use part of the 800-nm amplified beam and the OPA output as pump and prepump. Pump and prepump (probe) durations were 150 fs (30 fs), respectively. The samples consist of a GaAs layer ($d=0.65$ μm) sandwiched between two $0.2-\mu$m $Ga_{0.35}Al_{0.65}As$ layers grown

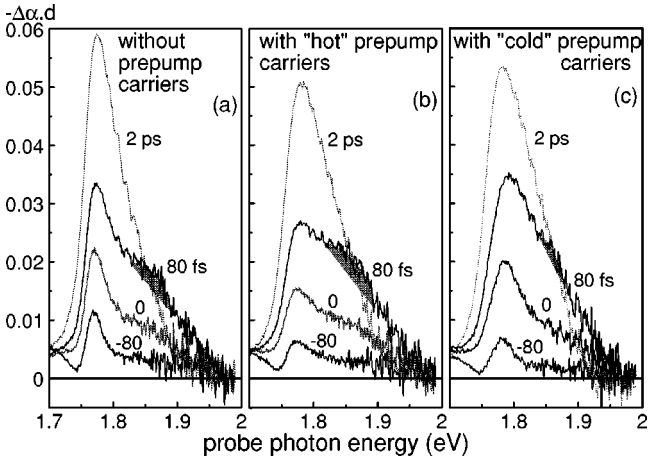

FIG. 1. Differential absorption spectra in undoped GaAs at 300 K in the presence [(b) and (c)] and in the absence of a prepump (a) for a pump energy of 1.544 eV (120 meV excess energy with respect to the band gap), and a prepump energy of 1.43 eV and for delay times: -80, 0, 80, and 2 ps. The prepump and pump-induced carrier density was estimated to be 8×10^{16} cm^{-3} and 3×10^{17} cm^{-3}, respectively. The pump-prepump delay was 2 ps in (b) and 300 fs in (c). The shaded areas are meant as a guide to the eye, helping to identify the differences between the three cases that are related to the electron populations.

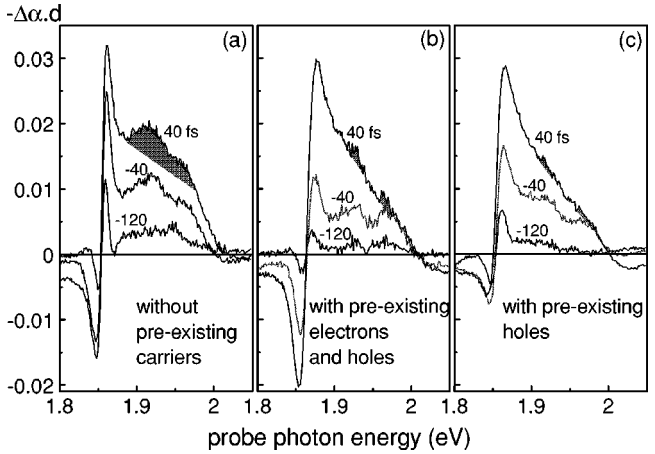

FIG. 2. Differential absorption spectra at 15 K in undoped GaAs in the absence (a) and in the presence of a prepump (b), and in *p*-doped GaAs $p=7\times10^{16}$ cm^{-3} (c) for a pump energy of 1.607 eV (88 meV excess energy) and for delay times: -120, -40 fs, and 40 fs. The pump-induced (prepump) carrier density was 10^{17} cm^{-3}(5×10^{16} cm^{-3}).

by molecular-beam epitaxy and antireflection-coated on both sides. The GaAs layer was either undoped or Be-doped. The samples are held at 15 K on the cold finger of a He-compressor cryostat or at room temperature. Hall measurements yielded (after corrections for the depletion layer), for the *p*-type sample, $p=7\times10^{16}$ cm^{-3} at 15 K and $p=5\times10^{17}$ cm^{-3} at 300 K.

In order to elucidate the role of the temperature of equilibrium carriers on the nonequilibrium carrier relaxation, we performed experiments with a low-excess-energy prepump in a room temperature lattice. The cold carriers created by the prepump heat up by phonon absorption and eventually reach the lattice temperature within 2 ps.[13] We can thus follow the evolution of nonequilibrium electrons in the presence of *cold* or *hot* preinjected electron-hole pairs, the rest of the experimental conditions being identical. If the nonequilibrium carriers are injected immediately after the carriers created by the prepump, the latter will still be ''cold.'' After 300 fs, the prepump-injected electrons have already thermalized and can be described with a Fermi-Dirac distribution with a temperature of about 200 K. On the other hand, if the nonequilibrium carriers are injected at a later time (2 ps later), the carriers created by the prepump will have reached the lattice temperature (300 K).

The differential absorption spectra are shown in Fig. 1 for a pump-prepump delay of 2 ps in (b), and of 300 fs in (c), and compared to the spectra in the absence of prepump (a). A shutter is placed in the optical path of the pump, and the quantity measured is $-\Delta\alpha d=-(\alpha_{p,pp}-\alpha_{pp})d$ where $\alpha_{p,pp}$ is the absorption in the presence of the pump and the prepump and α_{pp} the absorption in the presence of the prepump only. Thus, this experiment monitors the evolution of the pump-injected electrons while the signal due to the prepump-injected electrons is subtracted away.[14] The density of prepump-excited carriers remains constant during and after the pump pulse.

While the peaked structure on the low-energy side (1.76 eV) corresponds to the modifications of the $SO-C$ exciton due to many-body effects, the broad structure around 1.87 eV reflects the nonequilibrium electron populations photoexcited from the HH and LH valence bands. The two populations are not distinguished at room temperature. The comparison between Figs. 1(a) and 1(c) shows that *cold preinjected carriers accelerate the relaxation*: while in Fig. 1(a) for pump-probe delays of 80 fs, the peaked structure due to the pump-injected electrons is still visible, in Fig. 1(c) the nonequilibrium electrons have already completely redistributed. On the contrary, when the preinjected carriers are hot [Fig. 1(b)], the relaxation is somewhat slowed down: the structure due to the nonequilibrium carriers is more prominent for the same delay time of 80 fs (see shaded areas). To provide a more quantitative estimate of this effect, we have normalized the areas of the spectra and taken the difference between the spectra at 80 fs and those at 2 ps, where the distributions have thermalized, for the three different cases. We then squared and spectrally integrated this difference to obtain the mean square deviation from the thermalized spectral shape. Indeed, cold (hot) prepump carriers induce a mean square deviation from the spectral shape at 2 ps that is 27% smaller (5% larger) than without the prepump.

In order to determine whether cold electrons or holes are predominantly responsible for the acceleration of the thermalization, we carried out experiments in *p*-doped GaAs at 15 K where only cold holes are present [Fig. 2(c)] and in the presence of a prepump where both cold holes and electrons [Fig. 2(b)] preexist when the pump arrives. (In this case, the prepump carriers are injected 600 ps before the pump and have already reached the lattice temperature.) In both cases, the thermalization of the pump-excited electrons is drastically accelerated with respect to the undoped and not preexcited sample [Fig. 2(a)]. The differential absorption spectra for a pump-probe delay of 40 fs correspond to practically thermalized electron populations in Figs. 2(b) and 2(c) while for the same delay time the electrons in Fig. 2(a) are still far from equilibrium. A thermalized electron distribution (T

=500 K) is reached for the delay time of 80 fs (not shown) in the presence of cold carriers, whereas in their absence this thermalized distribution is reached much later: at 200 fs. At 40 fs, the mean square deviation from the spectral shape of the thermalized distribution is four times smaller in the presence of the cold carriers. The effect is similar whether cold electrons are present or not, which means that *cold holes are predominantly responsible for accelerating the thermalization of nonequilibrium electrons*. On the other hand, measurements on the *p*-type sample at room temperature show only a small effect of the preexisting holes on the nonequilibrium electron relaxation.

All these experimental observations are readily explained by considering the dynamically screened interaction potential between two carriers $V_S(q,\omega)=V(q)/|\epsilon(q,\omega)|$, where $V(q)$ is the bare Coulomb potential and $\epsilon(q,\omega)$ the retarded dielectric function. Obviously, strong scattering is observed for frequencies $\Omega(q)$ for which $\mathrm{Re}\,\epsilon[q,\Omega(q)]=0$ and $\mathrm{Im}\,\epsilon[q,\Omega(q)]\approx 0$, i.e., when plasma oscillations are excited. The first equality governs the plasmon dispersion $\Omega(q)$, whereas the second guarantees low damping Γ of the plasmon(s), $[\Gamma(q)\approx \mathrm{Im}\,\epsilon/[d\,\mathrm{Re}\,\epsilon/d\omega]|_{\omega=\Omega(q)}]$, e.g., Ref. 16. For bulk e-h plasmas in equilibrium only one weakly damped (optical) plasmon exists. For nonequilibrium distributions f with several maxima, additional undamped plasmons have been predicted which have a phase velocity $v_{ph}\approx\Omega/q$, corresponding to acoustic modes.[3,4] To estimate their damping, we compute ϵ in the random-phase approximation, $\epsilon(q,\omega)=1-V(q)\Sigma_a\Pi_a(q,\omega)$, where Π_a is the Lindhard polarization function $(a=e,h)$ the imaginary part of which is[10]

$$\mathrm{Im}\Pi_a(q,\omega)=-\frac{1}{2\pi\hbar^2}\frac{m_a}{q}\int_{k_a^-}^{k_a^+}dk k f_a(k), \qquad (1)$$

where $k_a^{\pm}=(m_a/\hbar^2 q)|\hbar\omega\pm E_a(q)|$, $E_a(q)=\hbar^2q^2/(2m_a)$, and the distributions are normalized according to $n_a=(1/\pi^2)\int_0^\infty dk k^2 f_a(k)$. The investigation of plasmons in multicomponent nonequilibrium systems is greatly simplified by considering the *velocity distributions* $F_a(v)\equiv m_a^2 v f_a(m_a v/\hbar)$. Expanding, in Eq. (1), F_a around $v=\omega/q$, yields, to order $O(q^2)$,

$$\mathrm{Im}\Pi_a(q,\omega)=-\frac{1}{2\pi\hbar^3}\left\{F_a\left(\frac{\omega}{q}\right)+\frac{\hbar^2q^2}{4m_a^2}\frac{d^2}{dv^2}F_a\left(\frac{\omega}{q}\right)\right\}.$$

This equation allows for a simple interpretation: The damping Γ of a plasmon with frequency ω and wave number q is essentially governed by the *total number of carriers N* moving with a velocity equal to its phase velocity, $N\sim F(\omega/q)\equiv\Sigma_a F_a(\omega/q)$, (cf. the first term in parentheses; the remaining terms become important only for large q). Thus, weakly damped acoustic plasmons are expected when the total velocity distribution $F(v)$ (i) has a minimum, and (ii) the minimum is deep. The analysis shows that the maximum number of acoustic modes is given by the number of minima of F, and their phase velocities fall into these minima.

Let us now consider the velocity distributions $F_a(v)$ for the experimental conditions. The nonequilibrium distribution functions $f_e(k)=f_h(k)$ (one average hole distribution function is used), were modeled as Gaussians with excess energy,

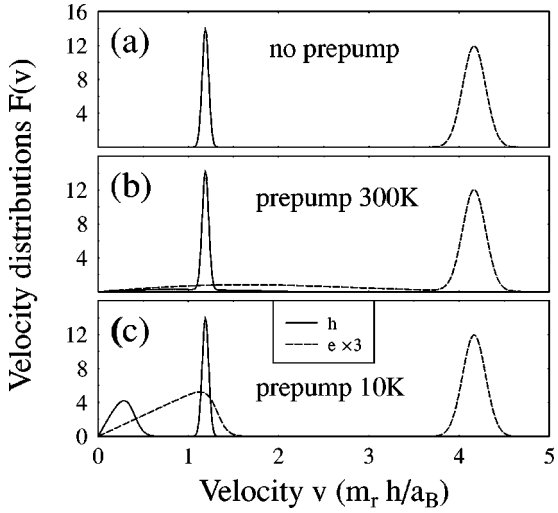

FIG. 3. Electron and hole velocity distributions corresponding to the prepump experiments (parameters as in Fig. 1; $E_R=4.2$ meV, $a_B=132$ Å, $m_e/m_r=1.284$, $m_h/m_r=4.5$, with m_r being the reduced mass).

spectral width and height determined by the pump pulse. Figures 3(a)–3(c) show the velocity distributions in the prepump experiments. Already the pump alone (a) generates a total distribution with a minimum, since, due to the different masses, the maxima of F_e and F_h are displaced with respect to each other. The addition of room temperature carriers (b) alters F only weakly. However, cold prepump-excited carriers (c) give rise to a second minimum between the cold thermal holes and the nonequilibrium holes. Based on the above analysis, we expect that, without prepump as well as with hot prepump carriers, there exists one weakly damped acoustic plasmon, while cold prepump carriers may allow for a *second acoustic mode* at lower phase velocity. Indeed, the numerical solution of the dispersion relation, $\mathrm{Re}\epsilon[q,\Omega(q)]=0$, confirms that, in all three cases, an acoustic plasmon is excited [see Fig. 4(a)]. Furthermore, room

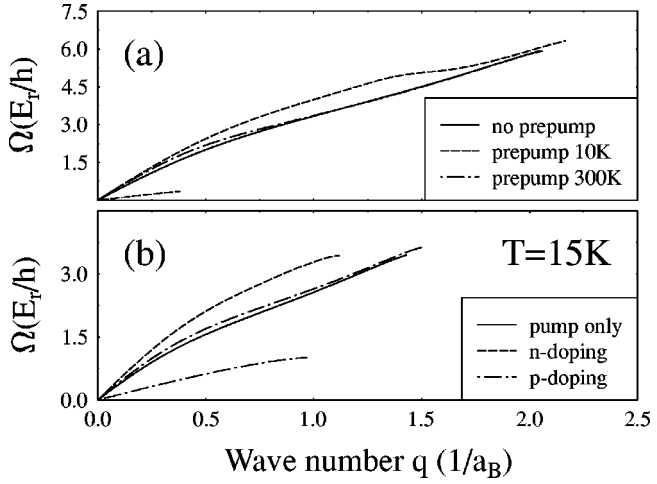

FIG. 4. Spectrum of acoustic plasmons in the presence/absence of preexisting thermal carriers. Part (a) shows the effect of a prepump (parameters as in Fig. 3) and (b) the influence of *p*- and *n*-doping (parameters as in Fig. 2, $n=p=5\times10^{16}\mathrm{cm}^{-3}$). In both figures, the lowest curve corresponds to the second acoustic plasmon.

temperature pre-excited carriers cause an increased damping due to thermal electrons ''leaking'' into the minimum of F, cf. Fig. 3(b), whereas, in contrast, low-temperature thermal carriers [Fig. 3(c)] allow for a *second acoustic plasmon*, thus yielding an additional efficient energy loss mechanism for the pump-excited carriers. With growing temperature of the prepump-induced carriers, the second minimum of $F(v)$ and, with it the second plasmon, gradually vanish.

In the experiments on the effect of doping, cold thermal holes and electrons both have a tendency to create a second minimum of the total distribution $F(v)$. However, thermal holes are much more favorable for acoustic plasmon undamping than electrons, since the low-velocity minimum of $F(v)$ is always broader and deeper in the case of holes [see Fig. 3(c)]. This is clearly confirmed from the analysis of the acoustic plasmon dispersion, Fig. 4(b). It turns out that *n*-doping leads to increased damping of the acoustic plasmon, whereas *p*-doping reduces the damping and, at low temperatures, gives rise to a second acoustic plasmon, the lowest curve in Fig. 4(b).[17] This directly explains the accelerated thermalization in samples containing cold thermal holes (see Fig. 2).

To further confirm our interpretation, we computed the carrier-carrier scattering rates, comparing static screening vs. dynamic screening, see, e.g., Ref. 10. In a static treatment, cold preexcited carriers tend to even slow down the thermalization due to increased Pauli blocking effects, whereas dynamic screening fully confirms the above predictions. The increased scattering rates found for dynamic screening in the presence of cold preexcited carriers lead to a faster redistribution of the pump-excited carriers as well as to a faster dephasing of the pump polarization and thus to a broader initial carrier distribution,[15] both resulting in faster thermalization. The reason why our explanation works, even without taking the excitation and relaxation dynamics into account, is that the acoustic plasmon spectrum $\Omega(q)$ is essentially determined by the *location* of the pump peaks of the distribution F, but only weakly depends on the peak width and pump-excited density (and hence on details of its time evolution and of the dephasing). Of course, to achieve quantitative agreement with the experiments, a full non-Markovian interband calculation will be required.

In conclusion, we have performed experiments which show evidence of nonequilibrium acoustic plasmons in 3D e-h plasmas. We demonstrated that preexisting cold thermal carriers (most importantly holes) may give rise to a second acoustic plasmon mode which strongly accelerates the thermalization of nonequilibrium carriers in bulk semiconductors.[18] Furthermore, we have shown that the experimental findings are well explained using a very simple and intuitive analysis of the shape of the total velocity distribution.

We are grateful to J.-P. Likforman and G. Rey for help with the OPA. M.B. acknowledges support from the DFG (Schwerpunkt ''Quantenkohärenz in Halbleitern'').

*Present address: IEMN-Dpt. ISEN, BP 69, 59652 Villeneuve d'Ascq Cedex, France.

[1] L. Chen, *Waves and Instabilities in Plasmas* (World Scientific Publishing Co. Pte. Ltd., Singapore, 1987).

[2] W. Sha, A.L. Smirl, and W.F. Tseng, Phys. Rev. Lett. **74**, 4273 (1995); G.C. Cho, T. Dekorsy, H.J. Bakker, R. Hövel, and H. Kurz, *ibid.* **77**, 4062 (1996).

[3] D.C. Scott, R. Binder, and S.W. Koch, Phys. Rev. Lett. **69**, 347 (1992).

[4] K. ElSayed, R. Binder, D.C. Scott, and S.W. Koch, Phys. Rev. B **47**, 10 210 (1993); D.C. Scott, R. Binder, M. Bonitz, and S.W. Koch, *ibid.* **49**, 2174 (1994).

[5] W.H. Knox, D.S. Chemla, G. Livescu, J.E. Cunningham, and J.E. Henry, Phys. Rev. Lett. **61**, 1290 (1988).

[6] L.H. Acioli, M. Ulman, F. Vallée, and J.G. Fujimoto, Appl. Phys. Lett. **63**, 666 (1993).

[7] U. Hohenester, P. Supancic, P. Kocevar, X.Q. Zhou, W. Kütt, and H. Kurz, Phys. Rev. B **47**, 13 233 (1993).

[8] J.A. Kash, Phys. Rev. B **51**, 4680 (1995).

[9] F.X. Camescasse, A. Alexandrou, D. Hulin, L. Bányai, D.B. Tran Thoai, and H. Haug, Phys. Rev. Lett. **77**, 5429 (1996); F.X. Camescasse, A. Alexandrou, and D. Hulin, Phys. Status Solidi B **204**, 293 (1997).

[10] R. Binder, D. Scott, A.E. Paul, M. Lindberg, K. Henneberger, and S.W. Koch, Phys. Rev. B **45**, 1107 (1992).

[11] L. Bányai, Q.T. Vu, B. Mieck, and H. Haug, Phys. Rev. Lett. **81**, 882 (1998); Q.T. Vu, L. Bányai, H. Haug, F.X. Camescasse, J.-P. Likforman, and A. Alexandrou, Phys. Rev. B **59**, 2760 (1999).

[12] M.K. Reed, M.K. Steiner-Shepard, and D.K. Negus, Opt. Lett. **19**, 1855 (1994).

[13] J.-F. Lampin, F. X. Camescasse, V. Thierry-Mieg, and A. Alexandrou, *Ultrafast Phenomena XI*, edited by W. Zinth, J. G. Fujimoto, T. Elsaesser, and D. Wiersma (Springer, Berlin, 1998).

[14] Note, however, that the prepump-induced electrons give some contribution to the differential absorption signal, through the modification of their distribution in the presence of the pump.

[15] A. Leitenstorfer, A. Lohner, T. Elsaesser, S. Haas, F. Rossi, T. Kuhn, W. Klein, G. Boehm, G. Traenkle, and G. Weimann, Phys. Rev. Lett. **73**, 1687 (1994).

[16] M. Bonitz, *Quantum Kinetic Theory* (Teubner, Stuttgart, 1998), Chap. 4.

[17] In the prepump case, the presence of thermal electrons leads to an increased damping of the second acoustic plasmon, compared to the *p*-doping case.

[18] It is expected that this effect will be even stronger in 2D and 1D, as there, the nonequilibrium acoustic modes may become unstable, cf. Ref. 16 and references therein.